

Research Paper

Lack of FGF21 promotes NASH-HCC transition via hepatocyte-TLR4-IL-17A signaling

Qianqian Zheng^{1,2}, Robert C. Martin¹, Xiaoju Shi³, Harshul Pandit¹, Youxi Yu³, Xingkai Liu³, Wei Guo⁴, Min Tan¹, Ou Bai⁴, Xin Meng⁵✉ and Yan Li¹✉

1. Department of Surgery, School of Medicine, University of Louisville, Louisville, KY 40202, USA.
2. Department of Pathophysiology, Basic Medicine College, China Medical University, Shenyang 110122, China.
3. Department of Hepatobiliary and Pancreatic Surgery, The First Hospital of Jilin University, Changchun 130021, China.
4. Department of Hematology, The First Hospital of Jilin University, Changchun 130021, China.
5. Department of Biochemistry and Molecular Biology, College of Life Science, China Medical University, Shenyang 110122, China.

✉ Corresponding authors: Xin Meng, Department of Biochemistry and Molecular Biology, College of Life Sciences; China Medical University, No. 77 Puhe Road, North New Area, Shenyang 110122, China. Phone: 86-24-23261440; E-mail: xmeng75@cmu.edu.cn; Yan Li, MD, PhD, Division of Surgical Oncology, Department of Surgery; University of Louisville School of Medicine, 511 S Floyd ST MDR Bldg Rm324, Louisville, KY 40202. Phone: 502-852-7107; E-mail: yan.li@louisville.edu.

© The author(s). This is an open access article distributed under the terms of the Creative Commons Attribution License (<https://creativecommons.org/licenses/by/4.0/>). See <http://ivyspring.com/terms> for full terms and conditions.

Received: 2020.03.13; Accepted: 2020.07.29; Published: 2020.08.07

Abstract

Rationale: Hepatocellular carcinoma (HCC) has been increasingly recognized in nonalcoholic steatohepatitis (NASH) patients. Fibroblast growth factor 21 (FGF21) is reported to prevent NASH and delay HCC development. In this study, the effects of FGF21 on NASH progression and NASH-HCC transition and the potential mechanism(s) were investigated.

Methods: NASH models and NASH-HCC models were established in FGF21 Knockout (KO) mice to evaluate NASH-HCC transition. IL-17A signaling was investigated in the isolated hepatic parenchymal cells, splenocytes, and hepatocyte and HCC cell lines.

Results: Lack of FGF21 caused significant up-regulation of the hepatocyte-derived IL-17A via Toll-like receptor 4 (TLR4) and NF- κ B signaling. Restoration of FGF21 alleviated the high NAFLD activity score (NAS) and attenuated the TLR4-triggered hepatocyte-IL-17A expression. The HCC nodule number and tumor size were significantly alleviated by treatments of anti-IL-17A antibody.

Conclusion: This study revealed a novel anti-inflammatory mechanism of FGF21 via inhibiting the hepatocyte-TLR4-IL-17A signaling in NASH-HCC models. The negative feedback loop on the hepatocyte-TLR4-IL-17A axis could be a potential anti-carcinogenic mechanism for FGF21 to prevent NASH-HCC transition.

Key words: Fibroblast growth factor 21; Nonalcoholic steatohepatitis; Toll-like receptor 4; IL-17A; Hepatocellular carcinoma

Introduction

Non-alcoholic fatty liver disease (NAFLD) encompasses a broad spectrum of conditions, ranging from non-progressive bland steatosis to nonalcoholic steatohepatitis (NASH) [1, 2]. NASH is the most severe form of NAFLD and a potential precursor of hepatocellular carcinoma (HCC) [3]. In previous studies, we found that hepatic fibroblast growth factor (FGF21) protein level increased in steatohepatitis but decreased during HCC development [4]. Severe NASH and aberrant pro-inflammatory

signaling were also found in the FGF21 knockout (FGF21KO) mice [5]. FGF21 is primarily produced in the liver under metabolic stress caused by starvation, hepatosteatosis, obesity and diabetes [6, 7]. Under the regulation of peroxisome proliferator-activated receptor α (PPAR α) in response to the accumulation of lipids, hepatic FGF21 elicits metabolic benefits, in turn acting on the adipocytes of distal adipose tissue, through the transmembrane receptor FGFR1-coreceptor β -Klotho complex [8]. This major

endocrine action of FGF21 results in a combination of effects including control of lipolysis, clearance of excessive free fatty acids (FFAs), enhancing expenditure of the stored lipid energy by mitochondrial substrate oxidation, catabolism and uncoupling, and therefore, negatively regulating hepatic or tissue steatosis, and adiposity [9, 10].

Pharmacological application of FGF21 holds great promise as an effective therapeutic means for treating obesity and diabetes [11-13]. Using native FGF21, FGF21 analogues or metformin to stimulate FGF21 production, several experimental studies have also implicated the metabolic bioactivities of FGF21 against NAFLD [14-16]. In a recent study, FGF21 is found to alleviate inflammation by suppression of T helper 17 (Th17) cell differentiation and IL-17A expression via regulation of adiponectin in a NASH mouse model [17]. Other studies have also shown that FGF21 exerts anti-inflammatory efficacy in down-regulation of the Th17-IL-17 axis in experimental models of rheumatoid arthritis [18, 19]. In clinical patients, the transition from steatosis to NASH has been demonstrated to be associated with hepatic infiltration of IL-17A-producing cells [20]. Accumulating evidence indicated that Th17-IL-17 axis mediates the progression from NASH to HCC [21, 22], while blockage of Th17-IL-17 axis can inhibit this progression [23]. All the previous studies build upon the scientific premise that FGF21 is a promising candidate for treating NASH and preventing NASH-HCC transition. However, the mechanism of FGF21, especially its effect on Th17-IL-17 axis during in NASH-HCC transition, has not been well addressed.

Currently, it is speculated that FGF21 may play an anti-inflammatory effect against NASH via inhibition of hepatic Th17 cell infiltration [18, 19, 23]. However, the liver is a tolerogenic organ with exquisite mechanisms of immune regulation that ensure upkeep of local and systemic immune tolerance to self and foreign insults [24]. Because of immune tolerance, hepatic Th17 cell infiltration and infiltrated cells-derived IL-17A production may be not the common scenario in NASH. As we know, Toll-like receptor 4 (TLR4) serves as an upstream signal of the Th17-IL-17 axis [25]. Recent studies have shown that TLR4 mediates inflammation in hepatic parenchymal cells and non-parenchymal cells in the early stages of NAFLD [26, 27], suggesting that the “liver cells” may contribute to the inflammatory events in liver tissue. Revealing the hepatic inflammatory mechanism is critical to help understand the potential anti-inflammatory/anti-cancer action of FGF21.

In this study, a NASH model and a NASH-HCC model were established in FGF21KO mice as well as the wild type controls. Administrations of exogenous

rhFGF21 and anti-IL17A antibody in mice were performed to investigate the anti-inflammatory mechanism of FGF21. Benign hepatocyte line and hepatoma cell lines were used to perform *in vitro* studies to explore the hepatocyte-based TLR4/IL-17A signaling and potential therapeutic targets against NASH-HCC transition. In addition, FGF21 and IL-17A expressions were determined in HCC patients, and analyzed using a web-based database, Gene Expression Profiling Interactive Analysis (GEPIA).

Results

Lack of FGF21 worsens the diet-induced NASH in mice

Based on the previous reports [28-30], methionine-choline deficient (MCD) diet-feeding for 2 weeks and 3 months would be optimal “study-windows” to assess the early and advanced lipid metabolic/inflammatory molecular events. In current study, the FGF21KO mice and WT mice were fed with high-fat MCD (HFMCDD) for 2 weeks and 3 months, respectively, while CD and HFD were used as controls. Steatohepatitis was defined in micro-sections with H&E staining, as evident by the pathological changes, and was confirmed by NAS system, which is well-accepted as a surrogate for the histologic diagnosis of NASH [31, 32]. Significant increases of serum ALT and TG as well as hepatic TG level were found in the FGF21KO mice with 3 months’ HFMCDD feeding, compared to all other groups. Consistently, the highest NAS was found in the FGF21KO mice with 3 months’ HFMCDD feeding, with statistical significance compared to all other groups. The highest NAS was rendered by inflammation score (Figure 1). Significantly up-regulated expressions of pro-inflammatory cytokines, especially the important components of Th17-IL-17A signaling, were found in FGF21KO-HFMCDD mice (Figure S1). The results indicated that lack of FGF21 could decrease the anti-inflammation potential in the liver during NASH development in the HFMCDD-fed mice.

Lack of FGF21 upregulates IL-17A, insulin-resistance and inflammation in NASH mice

IL-17A production and IL-17A-producing cells are accepted as key factors contributing to NASH development [33]. Considering the etiology and pathology of the Th17-IL-17A axis and its role in steatohepatitis, hepatic infiltration of IL-17A-producing cells was first determined. Subpopulations of CD4⁺/IL-17⁺ cells and CD4⁺/Foxp3⁺ cells were detected by flow cytometry at very low levels in the

isolated cells from the liver tissues compared to that in extrahepatic splenocytes (Figure S2-S3). IL-17A expression and production were further determined in liver tissues. IL-17A mRNA expression was significantly upregulated in the FGF21KO HFMCD-fed mice with compared to those with either CD or HFD feeding (Figure 2A). Consistently, IL-17A protein production was significantly increased in the liver tissues of FGF21KO-HFMCD mice (Figure 2B). Up-regulation of fatty acid (FA) transport, FA oxidation, FA esterification and FA synthesis, were also found in the liver tissues of FGF21KO-HFMCD mice (Figure 2C). In NAFLD patients, it is reported that approximately 60% of hepatic lipid accumulation is derived from the re-esterification of plasma free FAs derived from lipolysis because of insulin resistance [34]. We further investigated the adipose tissues in terms of insulin-resistance and inflammation. Enlarged adipocytes widely distributed to the white adipose tissue (WAT) but decreased expression of insulin receptor substrate 1 (IRS1) were found in the FGF21KO mice with HFMCD or HFD feeding. Significantly increased neutrophils and macrophages identified by MPO and F4/80 staining and crown-like structures (CLSs), composed of macrophages surrounding dead or dying adipocytes, were found in the FGF21KO mice with HFMCD or HFD feeding. Consistently, significantly increased IL-17A expression was found in adipose tissues of FGF21KO mice with HFMCD or HFD feeding (Figure 2D). The results indicated that lack of FGF21 caused increases of IL-17A production and up-regulation of FA metabolism in liver, and increased the severity of insulin-resistance and inflammation in adipose tissue, in which the increased IL-17A production further induced neutrophil and monocyte recruitment toward inflammation sites [35]. Because the liver is considered a tolerogenic organ with the mechanisms for appropriate regulation of immune cells [36], finding resources of IL-17A production in a subpopulation of liver cells is important to understand the NASH mechanism in FGF21KO mice.

Lack of FGF21 up-regulated IL-17A production of hepatic parenchymal cells

Hepatocytes, Kupffer cells and extrahepatic splenocytes were isolated from liver and spleen to determine IL-17A production and IL-17A signaling. It was interesting to find that significantly increased IL-17A production was detected in hepatocytes, in addition to Kupffer cells and splenocytes from FGF21KO-HFMCD mice. The initiating cytokines, IL-23 and IL-6, for Th17 lineage [37] and the upstream signals (STAT3, ROR γ t, NF- κ B and TLR4) for IL-17A

were determined in the isolated subpopulations. Significantly up-regulated expressions of IL-23, IL-6, NF- κ B, and TLR4 were found in Kupffer cells and hepatocytes of FGF21KO-HFMCD mice, while up-regulated transcription factors of both STAT3 and ROR γ t for Th17 lineage were detected in the splenocytes of FGF21KO-HFMCD mice (Figure 3A). This result indicated that the IL-17A could be produced in FGF21KO-hepatocytes via cross-talk with extrahepatic splenocytes. To confirm, an indirect co-culture assay was performed using the isolated hepatocytes and splenocytes. Significantly up-regulated protein levels of IL-17A and NF- κ B were found in the FGF21KO-hepatocytes when co-cultured with splenocytes from FGF21KO-HFMCD mice, while treatment with either rhFGF21 or anti-IL-17 antibody significantly attenuated the up-regulated protein levels of NF- κ B and IL-17A (Figure 3B). TLR4-mediated inflammation played an important role in liver diseases [26, 27]. However, most previous studies emphasized the pathophysiological importance of TLR4 from non-parenchymal cells such as Kupffer cells/macrophages [38, 39] and hepatic stellate cells [40]. The aberrant TLR4 signaling from hepatocytes, which make up approximately two-thirds of total liver cell population (60%-70%), could be more deleterious but there was no such study previously. We further investigated TLR4 expression in the primary culture of hepatocytes from FGF21KO mice. Unlike the Kupffer cells, very low levels of TLR4 expression were detected in the hepatocytes from FGF21KO mice as well as WT mice. However, when the cells were challenged by FFA, a moderate increase of TLR4 was found in WT-hepatocytes, but a significant increase of TLR4 was found in FGF21KO-hepatocytes. TLR4 expression was also studied in a benign cell line of hepatocyte (FL83B cells) and an HCC cell line (Hepal-6 cells) using a shRNA assay to knock down (KD) the FGF21 gene. Similarly, FFA challenging caused significant increases of TLR4 in either FL83B-FGF21KD cells or Hepal-6-FGF21KD cells (Figure 3C). The results indicated that lack of FGF21 could leave the hepatocytes to become an important resource of IL-17A production, while FFA played an important role in contributing to hepatocyte-IL-17A production. On the other hand, IL-17A protein also worsened TLR4/NF- κ B/IL-17A signaling and lipid accumulation in hepatocytes, especially in the FGF21KD cells (Figure S4-S5). Because adipose-derived FFA was a major resource contributing to steatosis in NASH, a co-culture assay was performed to co-culture adipocytes with hepatocytes. Similar to FFA challenging, co-culture with LPS stimulated 3T3-L1 cells induced significant increases of IL-17A production in FL83B-FGF21KD,

Hepal-6 and Hepal-6-FGF21KD cells (Figure 3D), which implies that LPS-induced FFA release contributed IL-17A production in hepatocytes. To explore the regulatory mechanism of FGF21 on hepatocyte-TLR4 signaling, FL83B cells were challenged with LPS and treated with TAK242, an inhibitor of TLR4, and rhFGF21 to investigate TLR4 and the down-stream signals including NF- κ B and IL-17A. The results indicated that the LPS-induced increases of NF- κ B and IL-17A were attenuated by either TAK242 or rhFGF21 (Figure 3E). To confirm the participation of TLR4-NF- κ B signaling in IL-17A production, NF- κ B signaling was inhibited by (-)-parthenolide, an inhibitor of NF- κ B, to investigate IL-17A as well as ROR γ t, a master transcription factor of IL-17 expression, in either FL83B/FL83B-FGF21KD cells or Hepal-6/Hepal-6-FGF21KD cells. The results

showed that treatments with either (-)-parthenolide or rhFGF21 attenuated significantly the expressions of IL-17A and ROR γ t (Figure 4A). An *in vivo* study was also performed in FGF21OK mice treated with TAK242 to confirm the participation of TLR4-NF- κ B signaling in early NASH model (2 weeks). The results indicated that inhibition of TLR4 attenuated significantly the expressions of IKK α , IKK β , p-I κ B/I κ B, and p-NF- κ B/NF- κ B in the isolated hepatocytes from liver tissues of NASH model (Figure 4B). Interestingly, TAK242 treatment also attenuated significantly the expression of YAP (Figure 4C), an important component of HIPPO pathway. All the data evoked the interest to further study whether FGF21 could protect hepatocytes via negative feedback to the hepatocyte-derived IL-17A production, and thereby prevent NASH-HCC.

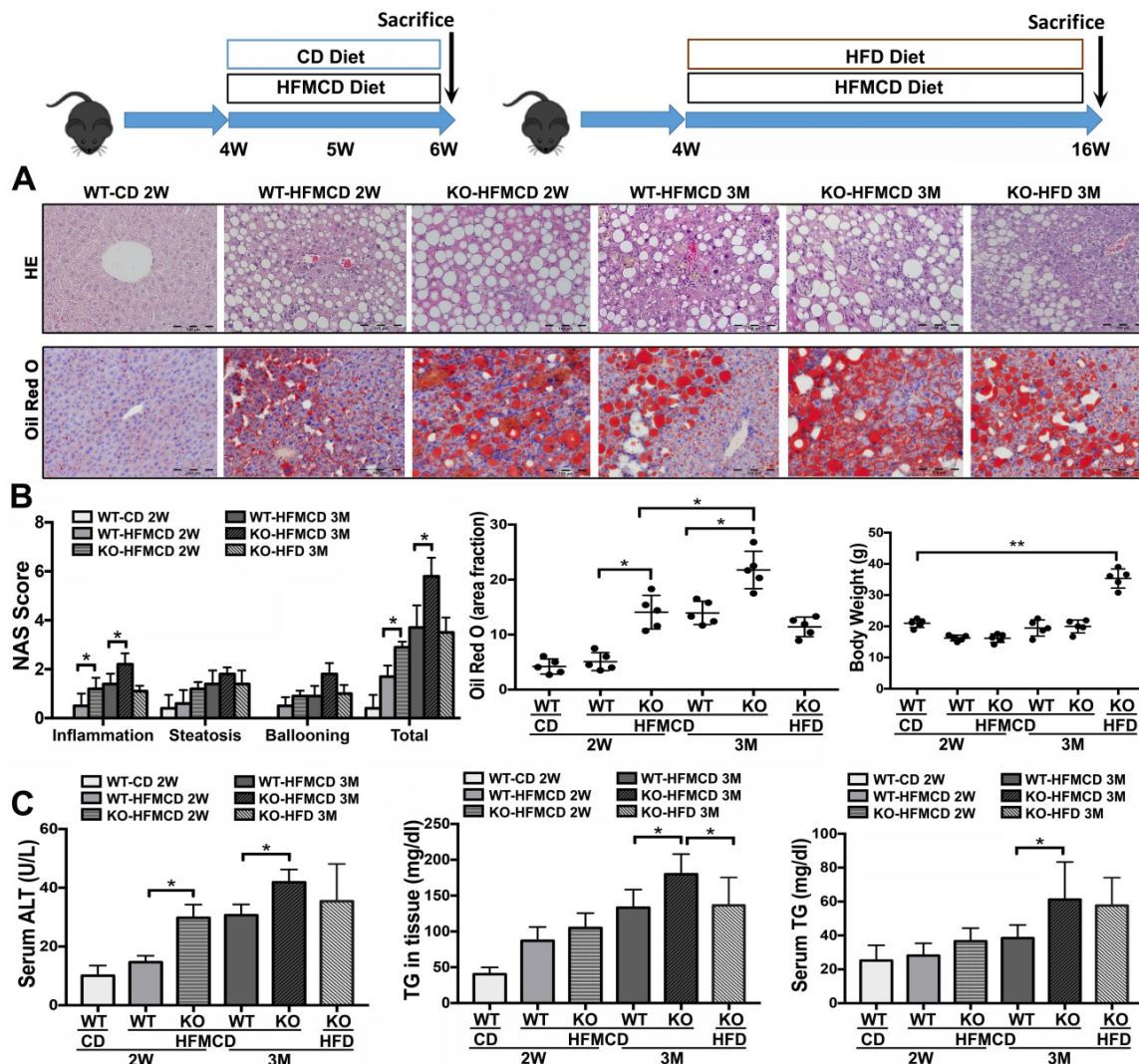


Figure 1. Establishing NASH models in FGF21KO mice. **A.** Representative histology by H&E and Oil Red O staining in the liver tissues from 4 groups (WT-CD; WT-HFMCD 2W; FGF21KO-HFMCD 2W; WT-HFMCD 3M; FGF21KO-HFMCD 3M; and FGF21KO-HFD 3M). For histological details in the H&E staining, bland steatosis was characterized as infiltration of inflammatory cells in the acinar zone and in the form of hepatocyte ballooning being detected. The Oil red O staining confirmed steatosis by identification of the lipid drops. **B.** NAFLD activity score (NAS), computer-imaging analysis for lipid drops of positive Oil Red O staining and Liver weight in all the study groups. NAS was calculated by the sum of scores of steatosis (0-3), lobular inflammation (0-3) and hepatocyte ballooning (0-2). The scoring is conducted as follows: Steatosis: 0, <5%; 1, 5-33%; 2, >33%; 3, > 66. Lobular Inflammation: 0, no foci; 1, <2 foci/200X; 2, 2-4 foci/200X; 3, >4 foci/200X. Hepatocyte Ballooning: 0, no balloon cells; 1, 1-5 balloon cells/200X; 2, >5 balloon cells/200X. **C.** Serum ALT, serum TG levels and hepatic TG levels in all the study groups. KO: FGF21KO; W: week; M: month. *, $P < 0.05$; **, $P < 0.01$.

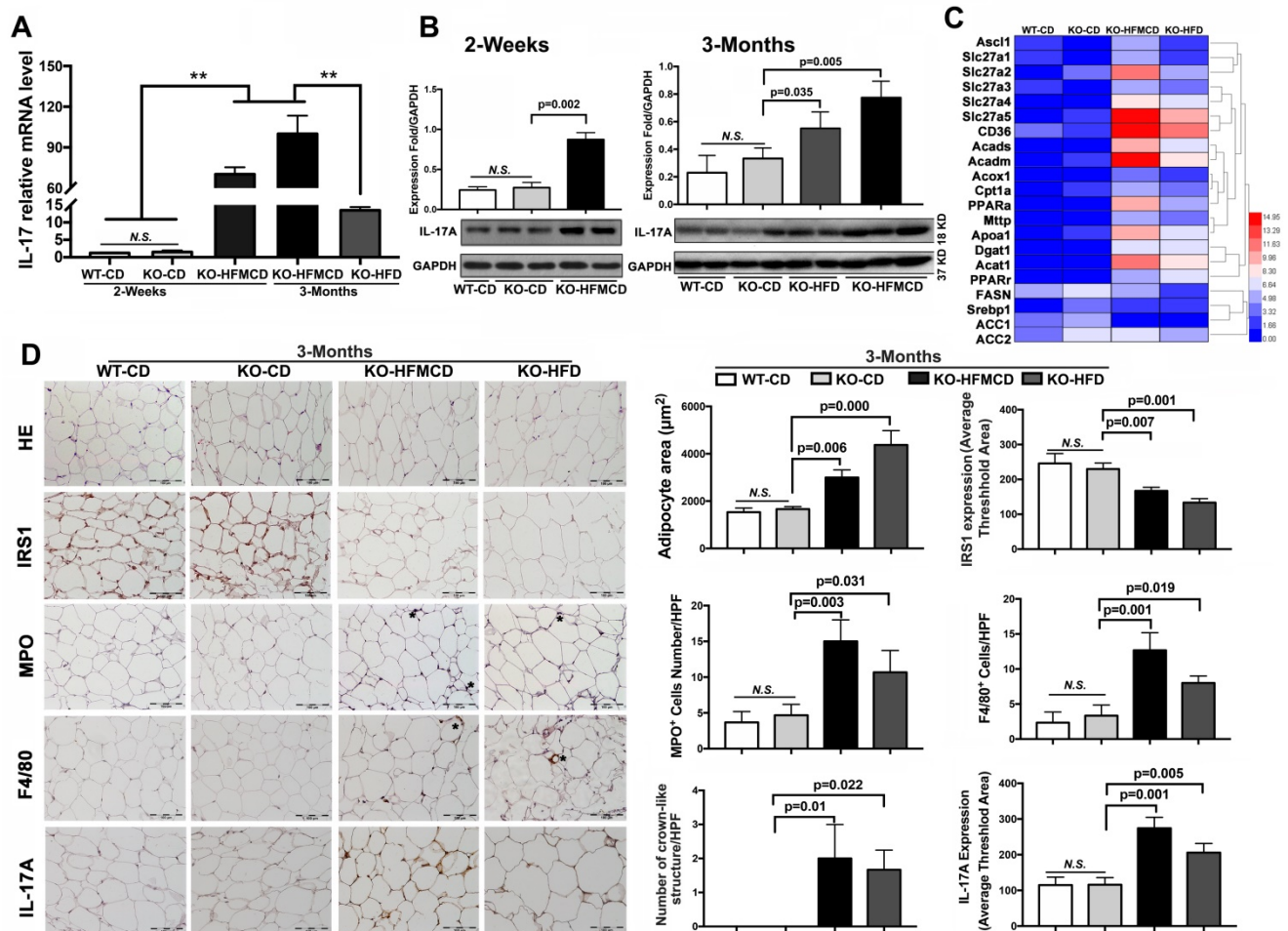


Figure 2. Aberrant IL-17A and insulin-resistance in NASH mice. **A,B.** The expressions of mRNA and protein levels of IL-17A from the liver tissues of FGF21 KO mice with HFMCD feeding for 2 weeks and 3 months as well as CD and HFD feeding controls. **C.** Heat map of FFAs metabolic signaling including FA transport (Ascl1, Slc27a1, Slc27a2, Slc27a3, Slc27a4, Slc27a5, and CD36), FA oxidation (Acads, Acadm, Acox1, Cpt1a, and PPARa), export (Mttp and Apoa1), esterification (Dgat1 and Acat1) and FA synthesis (FASN, Srebp1, ACC1, and ACC2) by q-PCR analysis in the FGF21KO mice with HFMCD feeding or HFD feeding for 3 months. **D.** Representative images of histology, IHC for IRS1, MPO, F4/80 and IL-17A, and computer-imaging quantification for the measurement of adipocyte area and the IHC expressions in the WAT from the FGF21KO mice with HFMCD feeding or HFD feeding for 3 months. Positive MPO cells and positive F4/80 cells as well as the number of crown-like structures were counted under microscope at high power field. HPF: high power field; KO: FGF21KO; **, $P < 0.01$.

rhFGF21 prevents NAHS via inhibition of the TRL4 mediated IL-17A production

In the early NASH model, alleviation of NASH pathology characterized by decreases of lipid accumulation and inflammatory infiltration in the liver tissues of mice with rhFGF21 treatment. Consistently, the NAS, hepatic TG and ALT were significantly decreased in mice with rhFGF21 treatment. Computer-imaging analysis in IHC showed significant decreases of IL-17A levels in liver tissues with rhFGF21 treatment ($P < 0.01$) (Figure 5A, B). Significantly down-regulated expressions of pro-inflammatory cytokines and IL-17A signaling and decreased Th17 cell/Treg cell ratio were found in FGF21KO-HFMCD mice with rhFGF21 treatment (Figure S6). The results indicated that restoration of FGF21 was critical in protecting the liver from the HFMCD insults in FGF21KO mice, while a decrease IL-17A might play a key role in hepatic protection.

Having determined the hepatic protection by rhFGF21, we next explored if restoration of FGF21 could modulate TLR4/NF-κB/IL-17A signaling in hepatocytes. In the isolated hepatocytes from 4 study groups, rhFGF21 treatment significantly attenuated the up-regulated protein levels of TLR4, NF-κB and IL-17A in the FGF21KO-HFMCD mice (Figure 5C). To further elucidate the effect of FGF21 on hepatocyte-TLR4 signaling, simvastatin (SIM), an inhibitor of the TLR4 signal, was used to treat the FL83B-FGF21KD and the Hepal-6-FGF21KD cells that were challenged with FFA. The results indicated that rhFGF21 was similar to SIM in attenuating the up-regulated expressions of TLR4, NF-κB and IL-17A (Figure 5D). Taken together, Inhibition of hepatocyte-IL-17A production could be an important mechanism for FGF21 to prevent NASH via a negative feedback loop on TLR4/NF-κB/IL-17A signaling.

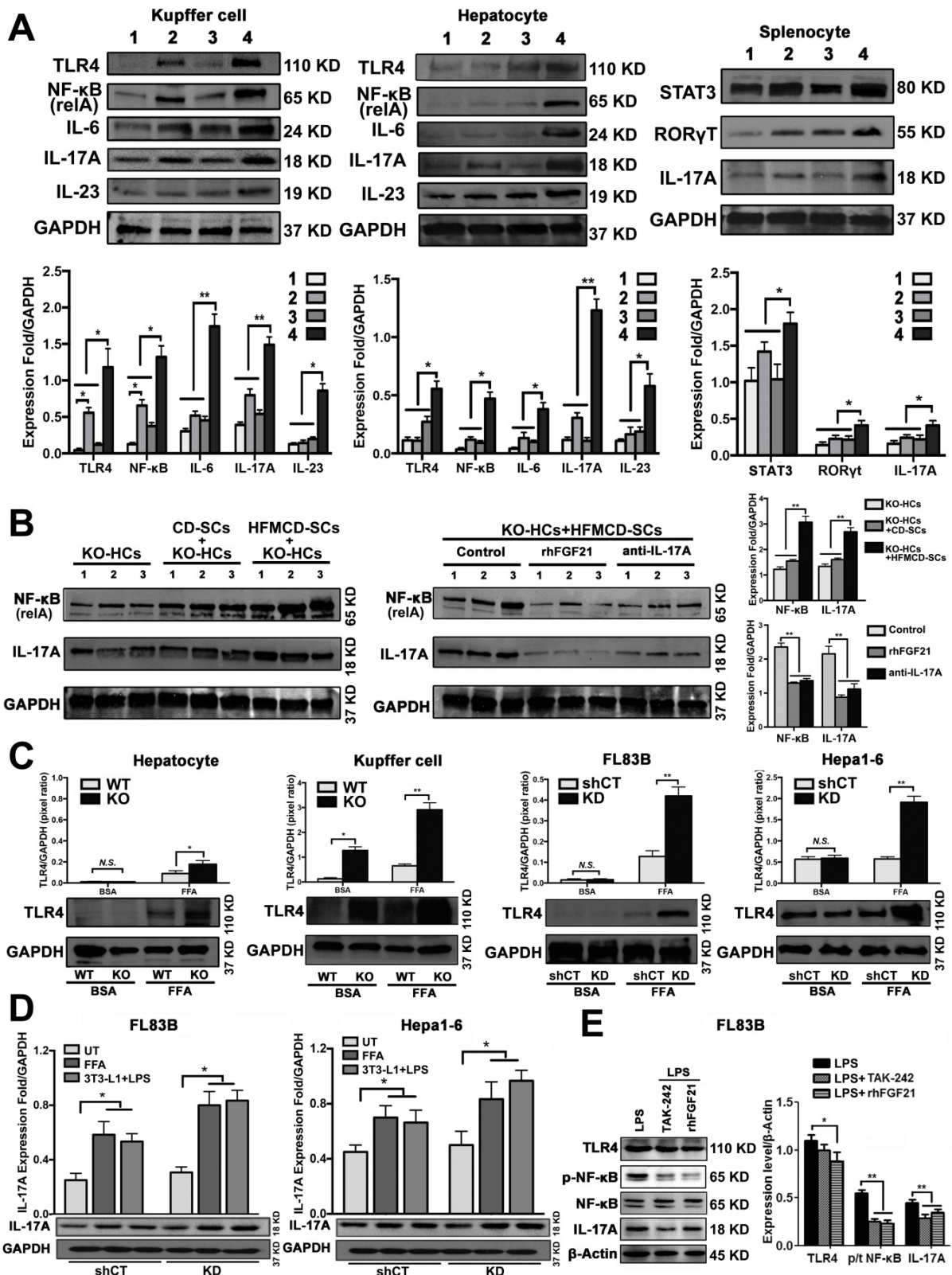


Figure 3. Up-regulated IL-17A production of hepatic parenchymal cells. **A.** Western blot analysis for the protein levels of TLR4, NF-κB (p65, relA), IL-17, IL-6, and IL-23 in the isolated Kupffer cells and hepatocytes as well as for the protein levels of STAT3, RORγT, IL-17 in the isolated splenocytes from early stage study groups (2 weeks) (1: WT-CD; 2: WT-HFMCD; 3: FGF21KO-CD; 4: FGF21KO-HFMCD). **B.** Western blot analysis for the protein levels of NF-κB and IL-17A in the FGF21KO-hepatocytes co-cultured with the splenocytes isolated from the spleens of FGF21KO-CD mice and FGF21KO-HFMCD mice. Monoclonal anti-mouse IL-17A antibody and rhFGF21 were used to treat the co-cultured cells at 100 ng/mL for 24 h. **C.** Western blot analysis for the protein levels of TLR4 in the primarily cultured hepatocytes and Kupffer cells (from the mice both FGF21KO and WT mice) as well as the hepatic cell lines (FL83B cells, Hepa1-6 cells, FL83B-FGF21KD cells and Hepa1-6-FGF21KD cells). The cells were challenged with FFA (palmitic acid) at 100μM for 48 h, 1% BSA was used as treatment control. **D.** Western blot analysis for the protein levels of IL-17A in the hepatic cell lines (FL83B cells and Hepa1-6 cells) and the associated cells of FGF21 gene knockdown by shRNA, named FL83B-FGF21KD cell and Hepa1-6-FGF21KD cell, which were co-cultured with adipocyte line, 3T3-L1 cells. **E.** Western blot analysis for the protein levels of TLR4, phosphorylated (p)-NF-κB, NF-κB (p65, relA), and IL-17A in FL83B cells challenged with LPS and treated with TAK-242 and rhFGF21. HCs: hepatocytes; SCs: splenocytes; KO: FGF21KO; KD: FGF21KD; FFA: free fatty acid; shCT: shControl. N.S.: no statistical significance; *, $P < 0.05$; **, $P < 0.01$.

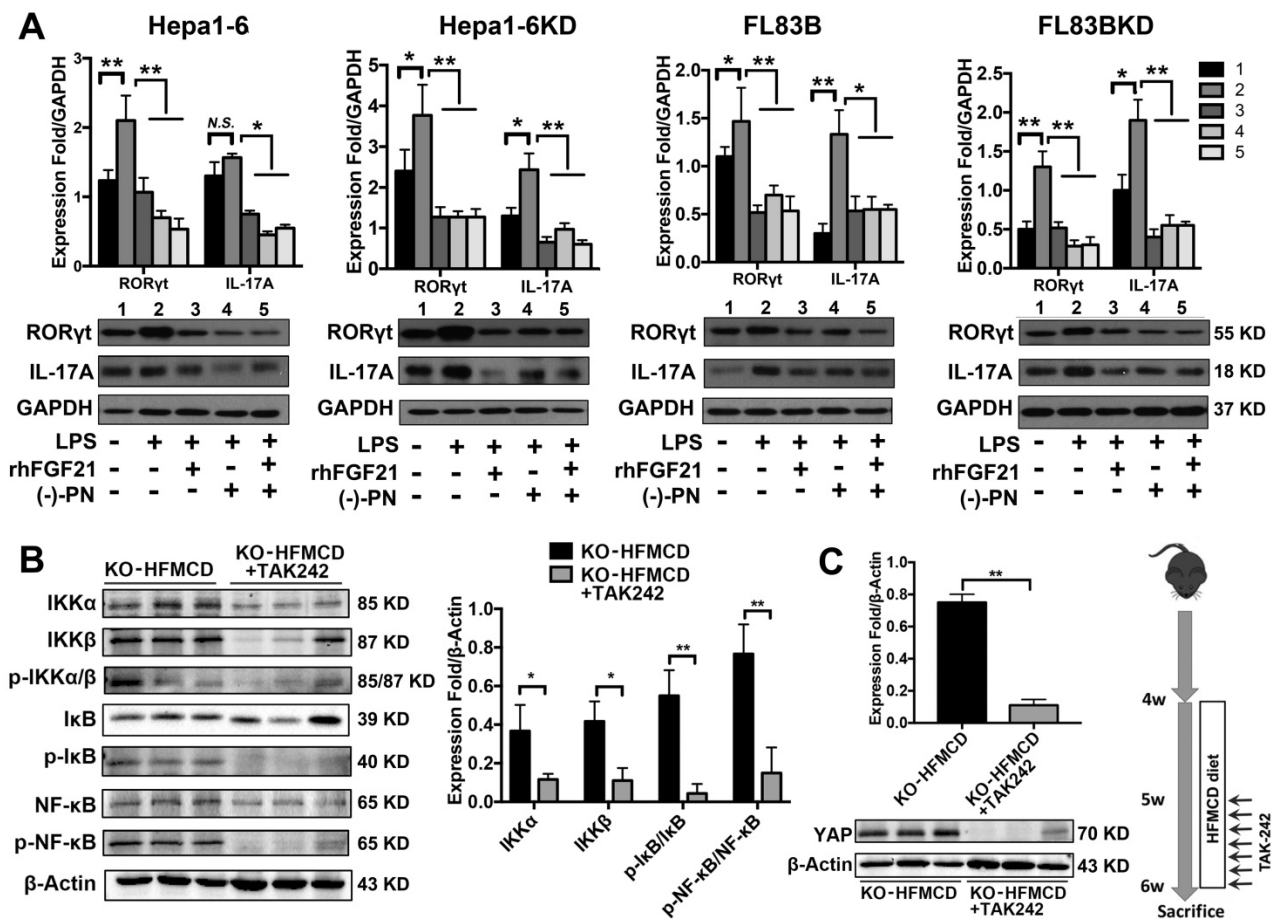


Figure 4. TLR4-NF-κB signaling contributed to IL-17A production and attenuation of IL-17A and YAP via inhibition of TLR4 in hepatocytes. **A.** Western blot analysis for the protein levels of RORγt and IL-17A in the FL83B/FL83B-FGF21KD cells and Hepal-6/Hepal-6-FGF21KD cells challenged with LPS and treated with (-)-parthenolide or rhFGF21. **B.** Western blot analysis for the protein levels IKKα, IKKβ, p-IκB/IκB, and p-NF-κB/NF-κB in the hepatocytes isolated from the FGF21KO-HFMCD mice and FGF21KO-HFMCD+TAK-242. **C.** Western blot analysis for the protein level of YAP in the hepatocytes isolated from the FGF21KO-HFMCD mice and FGF21KO-HFMCD+TAK-242. KO: FGF21KO; KD: FGF21 KD; FFA: free fatty acid; SIM: simvastatin; (-)-PN: (-)-parthenolide; N.S.: no statistical significance; * $P < 0.05$; ** $P < 0.01$.

Anti-IL-17A inhibits HCC progression in FGF21KO mice

Because IL-17A signaling was accepted as a crucial link for the transition from NAFLD to HCC [41], we further performed an anti-IL-17A treatment in a NASH-HCC transition model established by DEN injection followed by HFMCD/HFD feeding in FGF21KO mice (Figure S7). By ultrasound imaging, tumor nodule was detected at 6 weeks after DEN (2 weeks after HFMCD), while multiple and bigger nodules were detected at 16 weeks after DEN (12 weeks after HFMCD). No tumor nodule was detected in DEN+HFD mice. Based on the results of DEN+HFMCD versus DEN+HFD, the DEN+HFMCD model was selected and an anti-IL-17A treatment window was determined from 6 weeks to 16 weeks to assess its effect on NASH-HCC transition and HCC progression. All FGF21KO mice with DEN+HFMCD developed HCC at 16 weeks, however, lower burden of liver tumors was found in the mice with anti-IL-17A treatment. Macroscopically, smaller size and fewer numbers of HCC nodules were found in

the mice with anti-IL-17A treatment compared to the untreated mice. When a scatter plot was created with length and number of the HCC nodules to present tumor growth patterns, significantly alleviated tumor growth was found in anti-IL-17A treated mice compared to the untreated mice (Figure 6A). Decreased NAS was also found in the anti-IL-17A treated mice, with statistical significance compared to the untreated mice. The NAS result showed that the decreased total NAS was from the decreased score of inflammation other than steatosis and ballooning (Figure 6B), supporting the anti-inflammatory effect of anti-IL-17A. The HCC nodules were confirmed as HCC foci by the cytological features of cancerous cells; ranging from well to poorly differentiated; distributed in parenchyma showing an abnormal hepatic architecture. NASH pathology was further evidenced by lipid accumulation using Oil Red O staining and by fibrosis using Sirius Red staining (Figure 6C). Significant decreases of serum TG, ALT and AFP were found in the anti-IL-17A treated mice compared to the untreated mice (Figure 6D). Taken

together, lack of FGF21 accelerates the NASH-HCC transition via up-regulation of IL-17A signaling. FGF21 could be important in the protection of hepatocytes against NASH-HCC transition via a negative feedback loop on IL-17A signaling in hepatocytes.

Aberrant signaling of FGF21/ IL-17A /YAP in human HCC

The data from NASH-HCC mice suggested that the FGF21-IL-17A axis could play an important role during the NASH-HCC carcinogenetic process. Further study was performed in human HCC specimens. The protein levels of FGF21 and IL-17A were determined by ELISA assay in the HCC tissues

as well as the adjacent benign tissues. Significantly increased IL-17A was found in the HCC tissues compared to the adjacent benign tissues. In contrast, significantly decreased FGF21 was found in the HCC tissues compared to the adjacent benign tissues (Figure 7A). The IHC analysis was confirmed by the ELISA results (Figure 7B). We also determined the serum FGF21 and IL-17A by ELISA assay in the 8 HCC patients before and after HCC-nodule resection. The results indicated that the aberrant IL-17A levels were alleviated in 6 out of 8 patients, while the FGF21 levels were increased in all patients post-operatively (Figure 7C). To further identify the clinical relevance of FGF21 in human HCC, the survival rate of HCC patients associated with FGF21 expression was

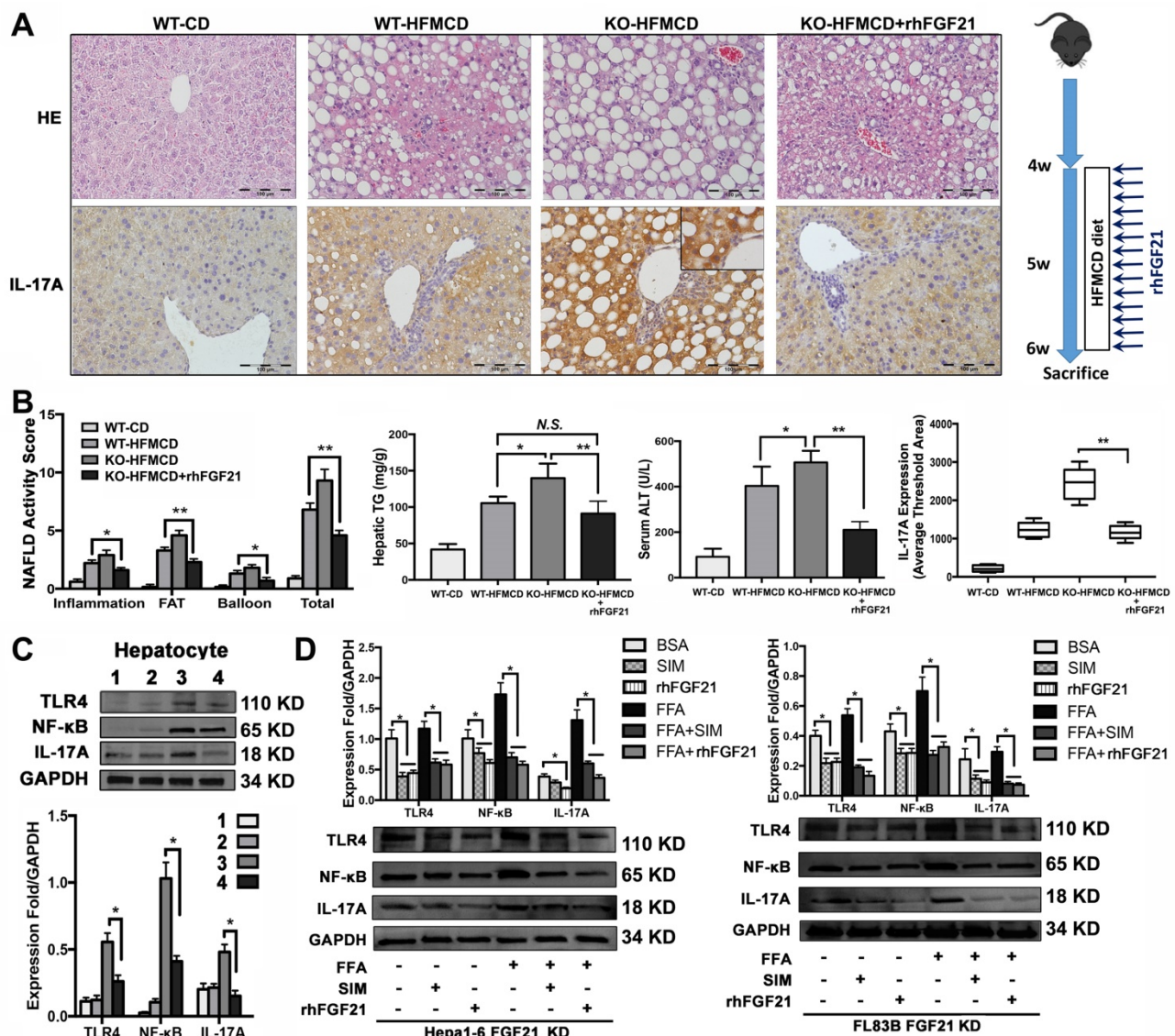


Figure 5. rhFGF21 preventing NAHS via inhibition of IL-17A production. **A.** Representative histology by H&E stain and IL-17 expression by IHC staining in the liver tissues from 4 groups (WT-CD; WT-HFMCd; FGF21KO-HFMCd; FGF21KO-HFMCd+rhFGF21). **B.** The NAFLD activity score (NAS), hepatic TG, serum ALT and computer-imaging quantification of IL-17 expression were determined in all 4 groups. NAS was calculated as aforementioned. **C.** Western blot analysis for the protein levels of TLR4, NF-κB, and IL-17A in the hepatocytes isolated from the 4 group mice (1: WT-CD; 2: WT-HFMCd; 3: FGF21KO-HFMCd; 4: FGF21KO-HFMCd+rhFGF21). **D.** Western blot analysis for the protein levels of TLR4, NF-κB and IL-17A in the FL83B-FGF21KD cells and Hepa1-6-FGF21KD cells treated with FFA, SIM and rhFGF21, respectively. KO: FGF21KO; KD: FGF21 KD; FFA: free fatty acid; SIM: simvastatin; N.S.: no statistical significance; *, $P < 0.05$; **, $P < 0.01$.

determined using a web-based database, Gene Expression Profiling Interactive Analysis (GEPIA). The results indicated that the high expression of FGF21 was positively correlated with a better prognosis in HCC patients (Figure 7D). IL-17A expression and carcinogenetic pathways in the GEPIA were further analyzed to explore the potential carcinogenetic signaling linked to the FGF21 and survival. When normalized by FGF21, survival curves showed a significant negative correlation with the mRNA levels of IL-17A, YAP and TAZ (both YAP and TAZ are the main components in the Hippo pathway) (Figure 7E-G). The mRNA levels of YAP and TAZ were further analyzed in HCC and non-tumor liver tissues using the GEPIA web tool. The results indicated that the YAP and TAZ mRNA levels were increased in LIHC (Liver hepatocellular carcinoma, n=369) compared to the normal sample (n = 50), while TAZ showed statistical significance but not YAP (Figure 7H). By co-expression analysis, there was a positive correlation between TAZ and FGF21 expression in LIHC ($R = 0.2$, $P < 0.001$) (Figure 7I). To confirm the data from GEPIA, IHC was performed using an anti-YAP/TAZ antibody in the HCC tissues as well as in adjacent benign tissues. The positive staining of YAP/TAZ was abundantly distributed in the nuclei of tumor cells in HCC tissues, however, abundantly distribution of YAP/TAZ was found in the cytosol of hepatocytes in adjacent benign tissues. Image-analysis showed significantly increased YAP/TAZ in nuclei, compared to the adjacent benign tissues (Figure 7J). Consequently, the important components (FASN, PPAR α , FGF21, IL-17A, IL-17RA, p-YAP TAZ and TLR4) related to the HCC carcinogenetic transformation were further evaluated by Western blot in the paired human samplers (malignant versus benign) of HCC patients. The results showed that upregulated protein levels (FASN, IL-17A, IL-17RA, p-YAP TAZ and TLR4) and downregulated protein levels (PPAR α and FGF21) were found in malignant tissues compared to the adjacent benign tissues (Figure 7K).

Discussion

In this study, we reported, for first time, that FGF21 plays a critical role for negative feedback on the hepatocyte-derived IL-17A production to attenuate NASH development and NASH-HCC transition. The major signaling components of the upstream and downstream signals of FGF21-IL-17A loop and the potential working hypothesis of FGF21 on NASH and NASH-HCC transition are shown as a schematic diagram in Graphical Abstract.

FGF21 is predominantly expressed in hepatocytes and can be induced under hepatic stress

[42]. Sufficient FGF21 not only directly reduces hepatic lipid accumulation in an insulin-independent manner [43, 44], but also inhibits the lipolysis of WAT and further decreases circulating FFAs levels [45]. All these metabolic bioactivities of FGF21 were considered to protect liver from the insults of the aberrant lipid accumulation. However, the metabolic benefits only were not enough to explain the therapeutic effect of FGF21 on NASH, which involved more progressive cellular events including inflammation, cell death and fibrosis progresses [46]. The liver is constantly exposed to toxic and microbial products, but no obvious damage occurs because a healthy liver can regulate inflammation and innate immune responses through protective signaling, such as the TLR signals; this protection is known as "liver tolerance"[24]. Breakdown of the liver tolerance may induce an inappropriate immune response, resulting in acute or chronic inflammatory liver diseases.

TLR4-mediated inflammation in liver cells serves an important role in NAFLD, however most previous studies focused on the TLR4 signaling in non-parenchymal cells such as Kupffer cells and hepatic stellate cells [26, 27]. Constituting over 60% of liver cells, hepatocytes are the principal site for the innate immune system to recognize the pathogen-associated molecules via pattern recognition receptors [47]. In our study, up-regulated TLR4 expression was found in the FGF21KO-hepatocytes, especially when the FGF21KO hepatocytes challenged by FFAs, suggesting a negative feedback role of FGF21 on the TLR4 signal in hepatocytes. While the hepatocyte-TLR4 is expressed at a very low levels and weakly responds to LPS and other inflammatory mediators [47, 48], the up-regulated TLR4 expression in FGF21KO-hepatocytes may be mediated by FFAs, which is supported by the followings: 1) Accumulation of FFAs in the liver causes hepatocyte injury by the intracellular FFA intermediates, such as diglycerides and ceramides, which are accepted as lipotoxic compounds via activation of TLR4[49]; 2) Because a major function of FGF21 is to prevent lipolysis [10], lack of FGF21 accelerates lipolysis to release FFAs which are accumulated in liver. Although the hepatocyte expressed TLR4 was not widely reported, the mRNA expression of hepatocyte-TLR4 was detected in the primary activated cultured hepatocytes and the hepatocyte-TLR4 was activated in responds to TLR4 ligands [50]. In addition, very low levels of TLR4 expression in hepatocytes have been reported in an *in vivo* study [51], which is consistent with our results detecting a low level of TLR4 in hepatocytes from WT mice. In FGF21KO-hepatocytes, however, a higher level of TLR4 expression was found and further up-regulated

in response to FFA challenging. rhFGF21 treatment attenuated the FFA-mediated TLR4-IL-17A signaling, rendering FGF21 an anti-inflammatory ability in addition to its metabolic activity. All these data indicated that FGF21 was indispensable for modulation of TLR4-IL-17A signaling to maintain “liver tolerance”.

Hepatocyte death [52] and activation of TLR4 [49] by lipotoxic intermediates are critical to initiate immune response and inflammation. It is considered that innate immune cells locate in non-lymphoid tissues where they are poised to respond immediately to tissue injury or pathogenic insults. Our results agreed with the general concept that Th17 cells could

develop from naïve CD4⁺ T cell precursors via cytokines to initiate cross-talk between liver cells and innate immune cells [53] in NASH, while a lack of FGF21 could accelerate this process. However, the FFA-mediated hepatocyte-TLR4 activation could be deleterious in clinical NASH patients but it had not been noted previously. The most important finding in the current study was the increased IL-17A via NF-κB in the hepatic parenchymal hepatocytes from FGF21KO mice with HFMCDD feeding. Comprising two-thirds of total liver cell population, hepatocytes could be an important resource contributing to IL-17A production, which was considered as a crucial link for NASH-HCC transition [41]. In our NASH-HCC

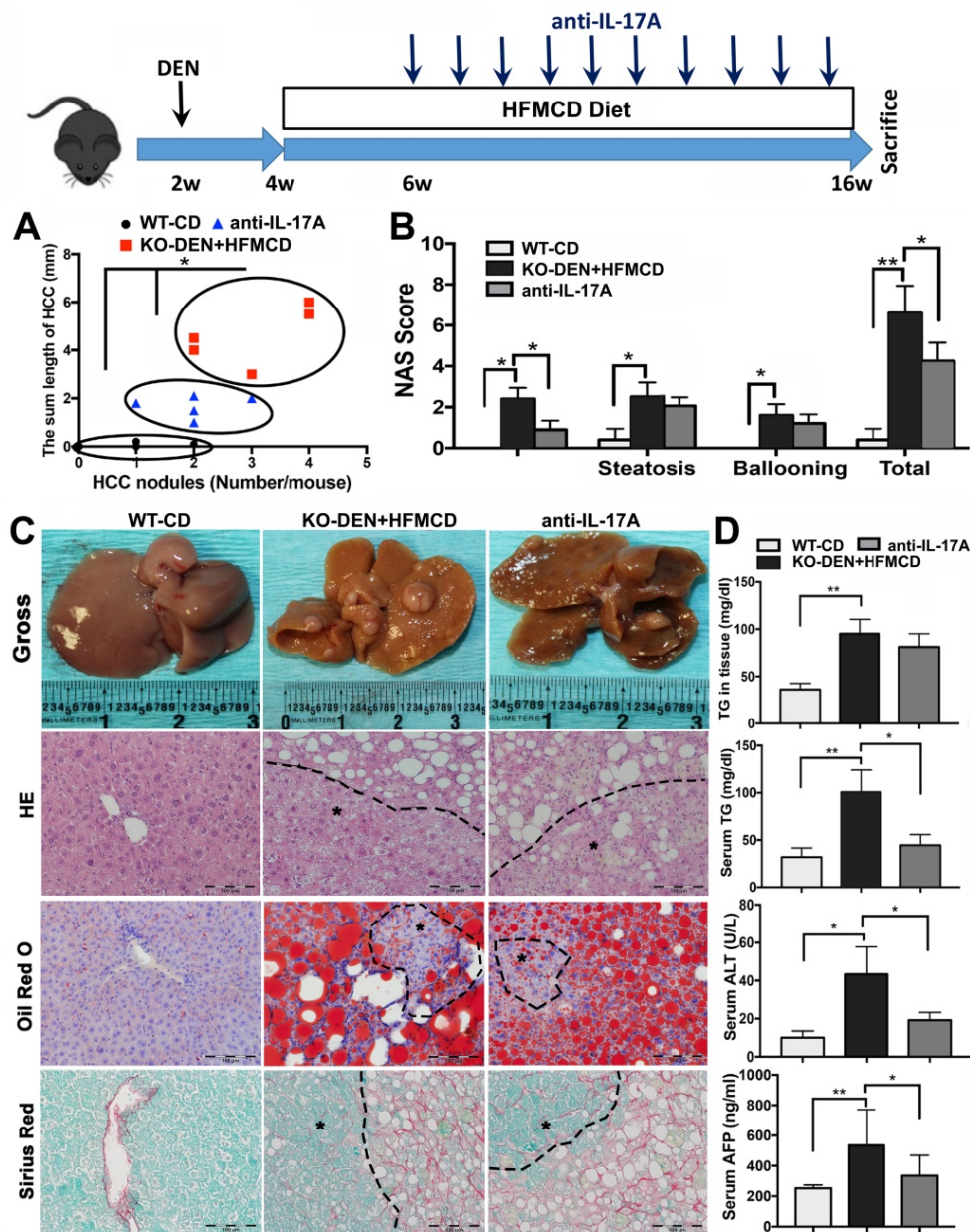


Figure 6. Anti-IL-17A inhibits NASH-HCC progression in FGF21KO mice. A. The NASH-HCC tumor growth pattern represented as the regression of HCC nodule length and HCC nodule numbers in individual HCC mouse. **B.** The NAFLD activity score (NAS). **C.** Representative gross anatomy of HCC nodules and histology by staining of H&E Oil Red O and Sirius Red in NASH-HCC mice with treatment of anti-IL-17A antibody. **D.** Hepatic TG levels, serum TG levels, serum ALT and serum AFP in the study groups. KO: FGF21KO; *, $P < 0.05$; **, $P < 0.01$.

model, an aggressive growth pattern of tumor nodules was detected in the FGF21KO mice with a single injection of DEN and HFMC feeding, while HCC lesions, in terms of nodule number and nodule size, was significantly alleviated when the animals were treated with anti-IL-17A antibody. All the data indicated that lack of FGF21 aggravated the TLR4-mediated up-regulation of IL-17A in hepatocytes, contributing to NASH-HCC transition. There could be a potential anti-carcinogenic mechanism for FGF21 via a negative feedback loop on the TLR4-IL-17A axis in the liver; this hypothesis was supported by the findings in which high expression of FGF21 and low

expression of IL-17A were closely correlated with better prognosis in the HCC patients. Based on the data from GEPIA and our HCC samples from clinical patients, the major components (YAP and TAZ) in HIPPO pathway were closely associated with the FGF21 and IL-17A expression levels in regard to the prognosis. Accumulating evidence suggests that HIPPO pathway plays a critical role linking the NASH-HCC transition [54-56]. Further study is needed to address the accurate role of YAP and TAZ, which could be important carcinogenic signaling involved in the NASH-HCC initiation and progression.

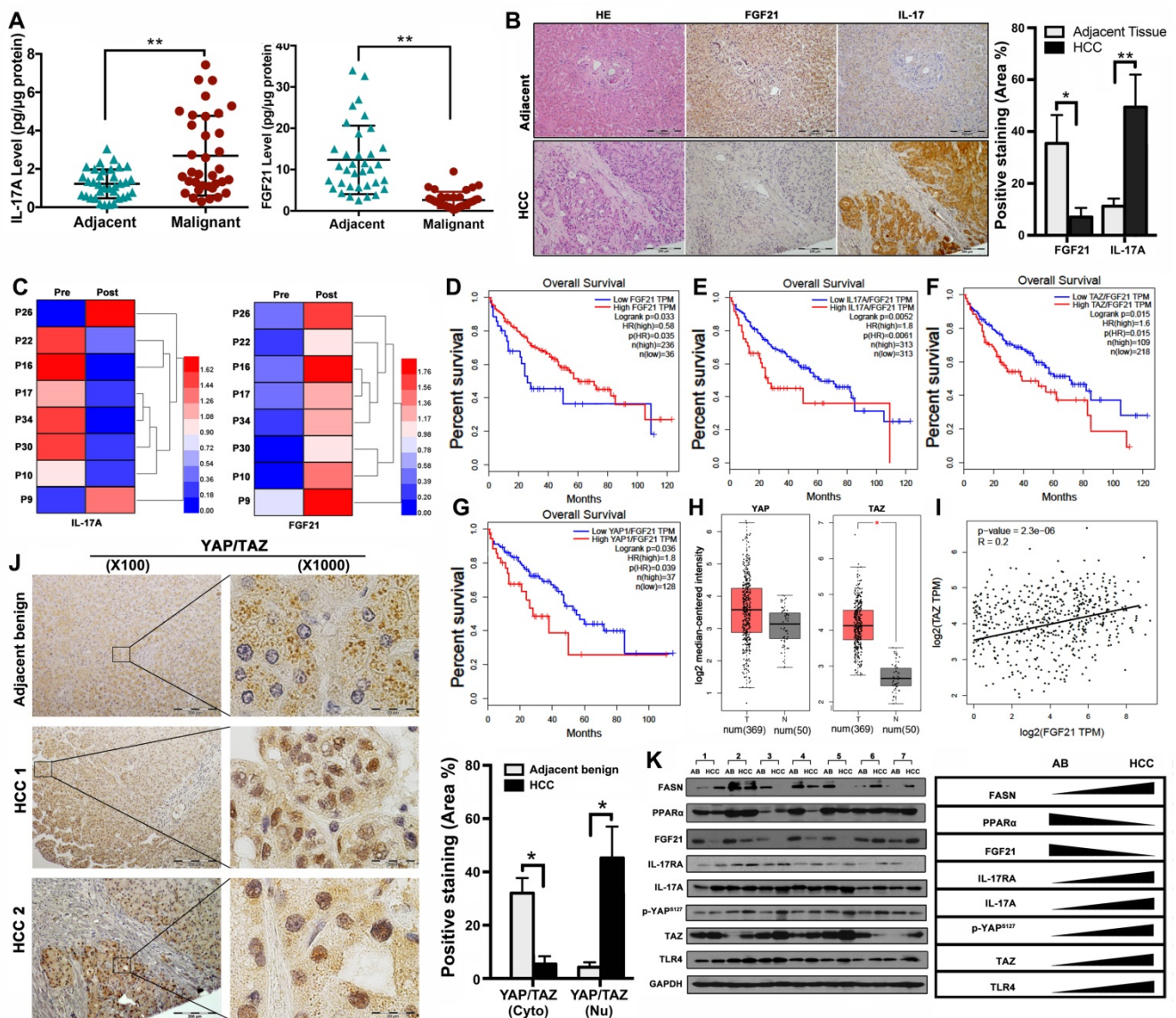


Figure 7. Aberrant signaling of FGF21/IL-17A/YAP in human HCC. **A.** Protein levels of IL-17A were analyzed by ELISA assay in HCC patients' malignant tissues as well as adjacent benign tissues. **B.** Representative histology by H&E staining and computer-imaging quantification of FGF21 and IL-17A expressions by IHC staining in patients' HCC tissues as well as adjacent benign tissues. **C.** Protein levels of IL-17A were analyzed by ELISA assay in patients' HCC pre-operation and post-operation. **D-G.** FGF21 mRNA expression levels and the FGF21 normalized YAP/TAZ/IL-17A mRNA expression levels in HCC patients associating with clinical outcomes. Low mRNA expression of FGF21 was correlation with poor prognosis in LIHC. High mRNA expression of IL-17A was correlation with poor prognosis in LIHC, as well as YAP and TAZ. Red, high expression; blue, low expression. **H.** \log_2 median-centered intensity of YAP expression and TAZ expression in the HCC patients (T) and Non-HCC patients (N). The GEPIA database revealed that TAZ expression was significantly upregulated in HCC. The boxplot analysis show \log_2 (TPM + 1) on a log-scale. T=369, N=50. **I.** The correlation between the mRNA expression levels of TAZ and FGF21 was determined in the TCGA-LIHC dataset analyzed using GEPIA. **J.** Representative images of YAP/TAZ distribution in cytosol and nuclear by IHC staining and computer-imaging quantification YAP/TAZ expressions in patients' HCC tissues as well as adjacent benign tissues. **K.** Western blot analysis for the protein levels of FASN, PPAR α , FGF21, IL-17A, IL-17RA, p-YAP^{S127}, TAZ, and TLR4 in patients' HCC tissues as well as adjacent benign tissues. AB: adjacent benign. *, $P < 0.05$; **, $P < 0.01$.

In conclusion, lack of FGF21 contributed to FFA-mediated induction of hepatocyte-TLR4 signaling to up-regulate IL-17A expression in hepatocytes. The potential anti-inflammatory effect of FGF21 could be through a negative feedback on the hepatocyte-TLR4 signaling to inhibit IL-17A production in the liver. The negative feedback loop on the hepatocyte-TLR4-IL-17A axis could be a potential anti-carcinogenetic mechanism for FGF21 to prevent NASH-HCC transition. This finding highlighted the potential pharmacological application of FGF21, especially for its anti-inflammatory effect, as a promising therapeutic strategy for clinical application to treat NASH at an early stage and thereby prevent NASH-HCC transition.

Materials and Methods

Establish NASH and NASH-HCC models

Male FGF21 Knockout (FGF21KO) mice with C57 BL/6J background were generously granted by Dr. Steve Kliewer (University of Texas Southwestern Medical Center). Wild-type (WT) C57 BL/6J mice were obtained from Jackson Laboratory (Bar Harbor, ME). For the NASH model, 4-week-old male mice were fed with HFMC (L-amino acid diet with 60 kcal% fat, 0.1% methionine and no added choline, A06071302, Research Diets, Inc., New Brunswick, NJ) for 2 weeks (early stage) or 3 months (advance stage), according to previous report [29, 30]. For the NASH-HCC model, male littermates, yielding the F1 generation, at 15 days of age received N-nitrosodiethylamine (DEN) (Sigma, St. Louis, MO) at 40 mg/kg by intraperitoneal injection (i.p.) according to our previous study [57]. When the mice with DEN administration were 4 weeks old, they were fed HFMC diet for 3 months. Control diet (CD, 10% kcal% fat, D12450B, Research Diets, Inc., New Brunswick, NJ) and high fat diet (HFD) (Rodent Diet with 60% kcal% fat, D12492, Research Diets, Inc., New Brunswick, NJ) were used. Treatments in animals were as follows: Recombinant human FGF21 (rhFGF21) (#100-42; PeproTech; Rocky Hill, NJ) was injected subcutaneously every day at 125 µg/kg bodyweight for 2 weeks; InVivoMab anti-mouse IL-17A (#BE0173, clone 17F3, Bio X Cell, Lebanon, NH 03766 USA) was injected intraperitoneally at 10 µg/kg bodyweight twice a week for 10 weeks. TAK-242 (Resatorvid, #614316, Millipore Sigma, MA), was injected intraperitoneally every day at 3 mg/kg bodyweight for 1 week. Six to eight mice were assigned in each group. The animal procedures were approved by the Institutional Animal Care and Use Committee of the University of Louisville, which is certified by the American Association for

Accreditation of Laboratory Animal Care.

Biochemical analysis, histology and NAFLD activity score

Serum alanine aminotransferase (ALT) was measured using an ALT Infinity Enzymatic Assay Kit (ThermoFisher Scientific Inc., Waltham, MA). Triglyceride (TG) was determined using a mouse Triglyceride Colorimetric Assay Kit (Cayman Chemical Company, CA). For histology, the harvested liver tissues were fixed in 10% buffered formalin for 2 weeks and then dehydration was done through graded alcohol series. The dehydrated tissues were cleared using xylene, embedded in paraffin, and sectioned at 4-5 µm slices. Hematoxylin and eosin (H&E) staining was performed in the micro-section to investigate the histopathological damage in the liver from all study groups. The images were reviewed and analyzed under microscope (Olympus 1X51, Olympus Corporation, Tokyo) at 20X magnification. The NAFLD activity score (NAS) was calculated from the sum of the individual scores for steatosis, inflammation and ballooning.

Cell isolation, cell culture, co-culture and treatments

Isolation of hepatocytes, Kupffer cells and splenocytes from liver and spleen tissues, establishment of Hepa1-6-FGF21KD cell and FL83B-FGF21KD cell, and method for 3T3-L1 cell differentiation are described in supplemental file. An indirect co-culture assay was performed for the isolated hepatocytes and splenocytes. In brief, the isolated hepatocytes were seeded at 1×10^5 in 24-well plate and cultured for 24 h in DMEM supplemented with 10% FBS and penicillin/streptomycin. The isolated splenocytes were pretreated with concanavalin A at 5 µg/mL to stimulate IL-17A and seeded at 1×10^4 in the insert of Transwell cell culture plates (Corning Incorporated, Corning, NY, USA). Then hepatocytes and splenocytes were co-cultured, without refreshing the medium, for 72 h. For FFA challenging, palmitic acid (PA) (Sigma-Aldrich, USA) at 100 µM was used to treat the cells, and 1% BSA was used as treatment control. To determine the effects of FGF21 and IL-17A antibody on cells, Recombinant Human FGF-21 (#100-42; PeproTech; Rocky Hill, NJ, USA) was used at 100 ng/mL, lipopolysaccharide (LPS, from Escherichia coli, Sigma Aldrich, USA) at 1 µg/mL, (-)-parthenolide (#S2341, Selleckchem, TX, USA) at 100 ng/mL, and InVivoMab anti-mouse IL-17A (#BE0173, clone 17F3, Bio X Cell, Lebanon) was used at 100 ng/mL to treat cell for 24 h. An assay was performed to co-culture indirectly the 3T3-L1 cells with the benign and malignant hepatic cell lines

(Hepa1-6 cells, FL83B cells, Hepa1-6-21KD cells and FL83B-21KD cells) using a Transwell plate. In brief, 3T3-L1 cells were differentiated up to 8 days, and then seeded at 1×10^5 in the insert of Trans-well plate for 24 h. After treatment with lipopolysaccharide LPS (Sigma Aldrich, USA) at $1 \mu\text{g}/\text{mL}$ for 12 h, the 3T3-L1 cells were co-cultured with hepatic cells for additional 24 h.

Human HCC tumor samples

The human HCC tissue samples were prospectively collected from 33 patients who had undergone HCC nodule resection along with corresponding adjacent benign tissues between 2002 and 2014 from the James Graham Brown Cancer Center Bio-Repository at the University of Louisville. The human HCC serum samples pre-operation and post-operation were collected from 8 patients at the hospital of the University of Louisville. A microscope examination of the cellular composition of hepatic tissue confirmed the diagnoses of HCC and benign on these liver tissues reviewed by two pathologists independently, blinded to the subject's clinical history. All the human sample collection procedures for this study were approved by the Institutional Review Board for Human Study at the University of Louisville.

GEPIA Database Analysis

Gene Expression Profiling Interactive Analysis (GEPIA), an online tool, was used to provide key interactions and functions based on the Cancer Genome Atlas (TCGA) and Genotype-Tissue Expression (GTEx) dataset for transcriptomic analysis (<http://gepia.cancer-pku.cn>) [PMID: 28407145]. In the GTEx dataset, the gene expression higher than median was defined as high expression group while the gene expression lower than median was defined as low expression group. By using the GEPIA tool, survival analyses were performed according to the gene expression levels of FGF21 and IL-17A using a log-rank test for hypothesis evaluation. GEPIA was further performed to determine a pairwise gene correlation analysis from any given set of TCGA and/or GTEx expression data using Pearson correlation statistics. The threshold was determined according to the following values: *P*-value of 0.01 and the hazard ration (HR) with 95% confidence intervals. Log-rank *P*-values were also calculated. The Spearman method was used to determine the correlation coefficient.

Statistical analysis

Collected data from repeated experiments were presented as mean \pm SD. Statistical analysis was performed by using SPSS V.17.0. Statistical

significance was determined by ANOVA. The post hoc Tukey's test was used for analysis of any differences between groups. Group difference was considered significant for $P < 0.05$ (*), $P < 0.01$ (**).

Supplementary Material

Supplementary figures and tables.

<http://www.thno.org/v10p9923s1.pdf>

Acknowledgments

We are grateful to Dr. Andrei Smolenkov at the James Graham Brown Cancer Center Bio-Repository (University of Louisville) for providing liver tumor specimens from patients.

Ethics approval and consent to participate

The animal procedures were approved by the Institutional Animal Care and Use Committee of University of Louisville, which is certified by the American Association for Accreditation of Laboratory Animal Care.

Funding

Research reported in this publication was supported partly by an Institutional Development Award (IDeA) from the NIGMS of the National Institutes of Health under grant number P20GM113226. The content is solely the responsibility of the authors and does not necessarily represent the official views of the National Institutes of Health.

Competing Interests

The authors have declared that no competing interest exists.

References

- Ballestri S, Nascimbeni F, Romagnoli D, Baldelli E, Targher G, Lonardo A. Type 2 Diabetes in Non-Alcoholic Fatty Liver Disease and Hepatitis C Virus Infection-Liver: The "Musketeer" in the Spotlight. *Int J Mol Sci.* 2016; 17: 355.
- Zoller H, Tilg H. Nonalcoholic fatty liver disease and hepatocellular carcinoma. *Metabolism.* 2016; 65: 1151-60.
- Marengo A, Rosso C, Bugianesi E. Liver Cancer: Connections with Obesity, Fatty Liver, and Cirrhosis. *Annu Rev Med.* 2016; 67: 103-17.
- Zhang Q, Li Y, Liang T, Lu X, Liu X, Zhang C, et al. Loss of FGF21 in diabetic mouse during hepatocellular carcinogenetic transformation. *American Journal of Cancer Research.* 2015; 5: 1762-74.
- Liu X, Zhang P, Martin RC, Cui G, Wang G, Tan Y, et al. Lack of fibroblast growth factor 21 accelerates metabolic liver injury characterized by steatohepatitis in mice. *American Journal of Cancer Research.* 2016; 6: 1011-25.
- Zhang F, Yu L, Lin X, Cheng P, He L, Li X, et al. Minireview: Roles of Fibroblast Growth Factors 19 and 21 in Metabolic Regulation and Chronic Diseases. *Molecular endocrinology.* 2015; 29: 1400-13.
- Nishimura T, Nakatake Y, Konishi M, Itoh N. Identification of a novel FGF, FGF-21, preferentially expressed in the liver. *Biochimica et biophysica acta.* 2000; 1492: 203-6.
- Fisher FM, Maratos-Flier E. Understanding the Physiology of FGF21. *Annual review of physiology.* 2016; 78: 223-41.
- Adams AC, Yang C, Coskun T, Cheng CC, Gimeno RE, Luo Y, et al. The breadth of FGF21's metabolic actions are governed by FGFR1 in adipose tissue. *MolMetab.* 2012; 2: 31-7.
- Inagaki T, Dutchak P, Zhao G, Ding X, Gautron L, Parameswara V, et al. Endocrine regulation of the fasting response by PPARalpha-mediated induction of fibroblast growth factor 21. *Cell metabolism.* 2007; 5: 415-25.

11. Foltz IN, Hu S, King C, Wu X, Yang C, Wang W, et al. Treating diabetes and obesity with an FGF21-mimetic antibody activating the betaKlotho/FGFR1c receptor complex. *Sci Transl Med.* 2012; 4: 162ra53.
12. Gaich G, Chien JY, Fu H, Glass LC, Deeg MA, Holland WL, et al. The effects of LY2405319, an FGF21 analog, in obese human subjects with type 2 diabetes. *Cell Metab.* 2013; 18: 333-40.
13. Kharitonov A, Beals JM, Coskun T, Dunbar JD, Hansen BC, Bumol TF, et al. Biological Profile of LY2405319, a Human FGF21 Variant and a Clinical Candidate. *Diabetes.* 2013; 62: A262-A.
14. Lee JH, Kang YE, Chang JY, Park KC, Kim HW, Kim JT, et al. An engineered FGF21 variant, LY2405319, can prevent non-alcoholic steatohepatitis by enhancing hepatic mitochondrial function. *Am J Transl Res.* 2016; 8: 4750-63.
15. Kim KH, Lee MS. FGF21 as a mediator of adaptive responses to stress and metabolic benefits of anti-diabetic drugs. *The Journal of endocrinology.* 2015; 226: R1-16.
16. Kim KH, Jeong YT, Kim SH, Jung HS, Park KS, Lee HY, et al. Metformin-induced inhibition of the mitochondrial respiratory chain increases FGF21 expression via ATF4 activation. *Biochemical and biophysical research communications.* 2013; 440: 76-81.
17. Bao L, Yin J, Gao W, Wang Q, Yao W, Gao X. A long-acting FGF21 alleviates hepatic steatosis and inflammation in NASH mice partly through an FGF21-adiponectin-IL17A axis. *Br J Pharmacol.* 2018.
18. Li SM, Yu YH, Li L, Wang WF, Li DS. Treatment of CIA Mice with FGF21 Down-regulates Th17-IL-17 Axis. *Inflammation.* 2016; 39: 309-19.
19. Yu Y, Li S, Liu Y, Tian G, Yuan Q, Bai F, et al. Fibroblast growth factor 21 (FGF21) ameliorates collagen-induced arthritis through modulating oxidative stress and suppressing nuclear factor-kappa B pathway. *International immunopharmacology.* 2015; 25: 74-82.
20. Rau M, Schilling AK, Meertens J, Hering I, Weiss J, Jurowich C, et al. Progression from Nonalcoholic Fatty Liver to Nonalcoholic Steatohepatitis Is Marked by a Higher Frequency of Th17 Cells in the Liver and an Increased Th17/Resting Regulatory T Cell Ratio in Peripheral Blood and in the Liver. *J Immunol.* 2016; 196: 97-105.
21. Gomes AL, Teijeiro A, Buren S, Tummala KS, Yilmaz M, Waisman A, et al. Metabolic Inflammation-Associated IL-17A Causes Non-alcoholic Steatohepatitis and Hepatocellular Carcinoma. *Cancer Cell.* 2016; 30: 161-75.
22. Giles DA, Moreno-Fernandez ME, Stankiewicz TE, Graspeuntner S, Cappelletti M, Wu D, et al. Thermoneutral housing exacerbates nonalcoholic fatty liver disease in mice and allows for sex-independent disease modeling. *Nat Med.* 2017; 23: 829-38.
23. Harley IT, Stankiewicz TE, Giles DA, Softic S, Flick LM, Cappelletti M, et al. IL-17 signaling accelerates the progression of nonalcoholic fatty liver disease in mice. *Hepatology (Baltimore, Md).* 2014; 59: 1830-9.
24. Crispe IN. Hepatic T cells and liver tolerance. *Nat Rev Immunol.* 2003; 3: 51-62.
25. Mu HH, Nourian MM, Jiang HH, Tran JW, Cole BC. Mycoplasma superantigen initiates a TLR4-dependent Th17 cascade that enhances arthritis after blocking B7-1 in Mycoplasma arthritis-infected mice. *Cell Microbiol.* 2014; 16: 896-911.
26. Kesar V, Odin JA. Toll-like receptors and liver disease. *Liver Int.* 2014; 34: 184-96.
27. Kiziltas S. Toll-like receptors in pathophysiology of liver diseases. *World Journal of Hepatology.* 2016; 8: 1354-69.
28. Du J, Zhang X, Han J, Man K, Zhang Y, Chu ES, et al. Pro-Inflammatory CXCR3 Impairs Mitochondrial Function in Experimental Non-Alcoholic Steatohepatitis. *Theranostics.* 2017; 7: 4192-203.
29. Matsumoto M, Hada N, Sakamaki Y, Uno A, Shiga T, Tanaka C, et al. An improved mouse model that rapidly develops fibrosis in non-alcoholic steatohepatitis. *Int J Exp Pathol.* 2013; 94: 93-103.
30. Tanaka N, Takahashi S, Zhang Y, Krausz KW, Smith PB, Patterson AD, et al. Role of fibroblast growth factor 21 in the early stage of NASH induced by methionine- and choline-deficient diet. *Biochimica et biophysica acta.* 2015; 1852: 1242-52.
31. Kleiner DE, Brunt EM, Van Natta M, Behling C, Contos MJ, Cummings OW, et al. Design and validation of a histological scoring system for nonalcoholic fatty liver disease. *Hepatology (Baltimore, Md).* 2005; 41: 1313-21.
32. Brunt EM, Kleiner DE, Wilson LA, Belt P, Neuschwander-Tetri BA, Network NCR. Nonalcoholic fatty liver disease (NAFLD) activity score and the histopathologic diagnosis in NAFLD: distinct clinicopathologic meanings. *Hepatology (Baltimore, Md).* 2011; 53: 810-20.
33. Ye P, Rodriguez FH, Kanaly S, Stocking KL, Schurr J, Schwarzenberger P, et al. Requirement of interleukin 17 receptor signaling for lung CXC chemokine and granulocyte colony-stimulating factor expression, neutrophil recruitment, and host defense. *J Exp Med.* 2001; 194: 519-27.
34. Marengo A, Jouness RI, Bugianesi E. Progression and Natural History of Nonalcoholic Fatty Liver Disease in Adults. *Clin Liver Dis.* 2016; 20: 313-24.
35. Chackelevicius CM, Gambaro SE, Tiribelli C, Rosso N. Th17 involvement in nonalcoholic fatty liver disease progression to non-alcoholic steatohepatitis. *World J Gastroenterol.* 2016; 22: 9096-103.
36. Lee GR. The Balance of Th17 versus Treg Cells in Autoimmunity. *Int J Mol Sci.* 2018; 19.
37. Yang XO, Panopoulos AD, Nurieva R, Chang SH, Wang D, Watowich SS, et al. STAT3 regulates cytokine-mediated generation of inflammatory helper T cells. *J Biol Chem.* 2007; 282: 9358-63.
38. Seki E, Tsutsui H, Nakano H, Tsuji N, Hoshino K, Adachi O, et al. Lipopolysaccharide-induced IL-18 secretion from murine Kupffer cells independently of myeloid differentiation factor 88 that is critically involved in induction of production of IL-12 and IL-1beta. *J Immunol.* 2001; 166: 2651-7.
39. Jin K, Liu Y, Shi Y, Zhang H, Sun Y, Zhangyuan G, et al. PIPROT aggravates inflammation by enhancing NF-kappaB activation in liver macrophages during nonalcoholic steatohepatitis. *Theranostics.* 2020; 10: 5290-304.
40. Inokuchi S, Tsukamoto H, Park E, Liu ZX, Brenner DA, Seki E. Toll-like receptor 4 mediates alcohol-induced steatohepatitis through bone marrow-derived and endogenous liver cells in mice. *Alcohol Clin Exp Res.* 2011; 35: 1509-18.
41. Hatting M, Tacke F. From NAFLD to HCC: Is IL-17 the crucial link? *Hepatology (Baltimore, Md).* 2017; 65: 739-41.
42. Yang C, Lu W, Lin T, You P, Ye M, Huang Y, et al. Activation of Liver FGF21 in hepatocarcinogenesis and during hepatic stress. *BMC gastroenterology.* 2013; 13: 67.
43. Lee J, Hong SW, Park SE, Rhee EJ, Park CY, Oh KW, et al. Exendin-4 regulates lipid metabolism and fibroblast growth factor 21 in hepatic steatosis. *Metabolism.* 2014; 63: 1041-8.
44. Li K, Li L, Yang M, Liu H, Boden G, Yang G. The effects of fibroblast growth factor-21 knockdown and over-expression on its signaling pathway and glucose-lipid metabolism *in vitro*. *Mol Cell Endocrinol.* 2012; 348: 21-6.
45. Chen W, Hoo RL, Konishi M, Itoh N, Lee PC, Ye HY, et al. Growth hormone induces hepatic production of fibroblast growth factor 21 through a mechanism dependent on lipolysis in adipocytes. *JBiolChem.* 2011; 286: 34559-66.
46. McPherson S, Hardy T, Henderson E, Burt AD, Day CP, Anstee QM. Evidence of NAFLD progression from steatosis to fibrosing-steatohepatitis using paired biopsies: implications for prognosis and clinical management. *Journal of Hepatology.* 2015; 62: 1148-55.
47. Schwabe RF, Seki E, Brenner DA. Toll-like receptor signaling in the liver. *Gastroenterology.* 2006; 130: 1886-900.
48. Mencin A, Kluge J, Schwabe RF. Toll-like receptors as targets in chronic liver diseases. *Gut.* 2009; 58: 704-20.
49. Gentile CL, Pagliassotti MJ. The role of fatty acids in the development and progression of nonalcoholic fatty liver disease. *J Nutr Biochem.* 2008; 19: 567-76.
50. Liu S, Gallo DJ, Green AM, Williams DL, Gong X, Shapiro RA, et al. Role of toll-like receptors in changes in gene expression and NF-kappa B activation in mouse hepatocytes stimulated with lipopolysaccharide. *Infect Immun.* 2002; 70: 3433-42.
51. Seki E, De Minicis S, Osterreicher CH, Kluge J, Osawa Y, Brenner DA, et al. TLR4 enhances TGF-beta signaling and hepatic fibrosis. *Nat Med.* 2007; 13: 1324-32.
52. Caballero F, Fernandez A, De Lacy AM, Fernandez-Checa JC, Caballeria J, Garcia-Ruiz C. Enhanced free cholesterol, SREBP-2 and StAR expression in human NASH. *Journal of Hepatology.* 2009; 50: 789-96.
53. Gaffen SL, Jain R, Garg AV, Cua DJ. The IL-23-IL-17 immune axis: from mechanisms to therapeutic testing. *Nat Rev Immunol.* 2014; 14: 585-600.
54. Ye J, Li TS, Xu G, Zhao YM, Zhang NP, Fan J, et al. JCAD Promotes Progression of Nonalcoholic Steatohepatitis to Liver Cancer by Inhibiting LATS2 Kinase Activity. *Cancer Res.* 2017; 77: 5287-300.
55. Fitamant J, Kottakis F, Benhamouche S, Tian HS, Chuvain N, Parachoniak CA, et al. YAP Inhibition Restores Hepatocyte Differentiation in Advanced HCC, Leading to Tumor Regression. *Cell Rep.* 2015; 10: 1692-707.
56. Guan C, Chang Z, Gu X, Liu R. MTA2 promotes HCC progression through repressing FRMD6, a key upstream component of hippo signaling pathway. *Biochemical and Biophysical Research Communications.* 2019; 515: 112-8.
57. Cui G, Martin RC, Jin H, Liu X, Pandit H, Zhao H, et al. Up-regulation of FGF15/19 signaling promotes hepatocellular carcinoma in the background of fatty liver. *Journal of Experimental & Clinical Cancer Research: CR.* 2018; 37: 136.